A Novel MMIC Active Filter with Lumped and Transversal Elements

MANFRED J. SCHINDLER, MEMBER, IEEE, AND YUSUKE TAJIMA, MEMBER, IEEE

Abstract — **A novel active filter structure has been developed and demonstrated as an MMIC. This filter structure makes use of both lumped elements and active transversal elements. The combination of lumped and transversal elements provides performance superior to that of a filter made of lumped elements alone and is much smaller than a filter made of transversal elements alone. This miniature MMIC filter has a passband of 9.8–11.1 GHz with 2 dB loss, and better than 30 dB rejection 1.1 GHz from either passband edge. This level of performance could not have been achieved on a conventional 4-mil-thick GaAs MMIC with only passive lumped elements.**

I. Introduction

MICROWAVE filters are generally realized with networks of distributed elements that can be quite large, or with discrete lumped elements which require custom tuning. For many applications, the size of distributed element filters is excessive. The cost of lumped element filters can be prohibitive. MMIC filters would offer the possibility of both small size and low cost.

The development of MMIC filters has received little emphasis, and the limited results that have been achieved have been disappointing. In general, MMIC filters are made with lumped capacitors and inductor equivalents (spiral inductors and/or high-impedance transmission lines). MMIC filters are typically only used where they are required as part of another function which is implemented on MMIC [1]. This is primarily attributable to the poor performance that may be expected of conventional MMIC filters.

Inductor equivalents on MMIC's are of relatively poor performance, regardless of whether they are spirals or high-impedance line sections. They suffer from both low Q and low self-resonant frequency. Spiral inductors typically have a Q of 30 at 10 GHz. The self-resonant frequency varies with inductor size; the largest value inductor that can practically be made with a self-resonant frequency below 18 GHz is on the order of 2 nH. Because of these limitations in inductor performance, filters with sharp cutoff characteristics cannot be realized. Somewhat better performance may be achieved if the substrate is thicker than the conventional 4 mils. Nonetheless, adequate filter response is generally unachievable.

The use of MMIC-compatible transversal and recursive filters has been reported. The size of a conventional transversal filter is excessive for a pure MMIC implementation. This has been circumvented by using an off-chip delay line [2]. The size of the complete filter assembly is still quite large. Novel topologies of transversal and recursive filters have also been shown [3]. These filters are smaller than conventional implementations, and could conceivably be implemented as MMIC's, although very large ones. An MMIC transversal filter implementation of a vector modulator has been demonstrated [4]. Since the objective was to achieve varying phase and amplitude, rather than filtering, a small monolithic realization was possible.

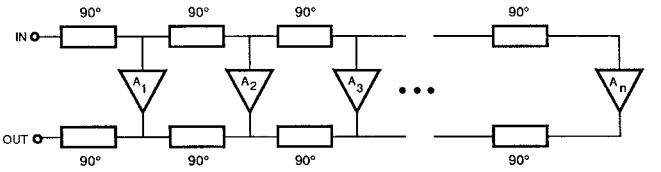

Fig. 1. Conventional microwave transversal filter structure.

The filter reported in this paper uses lumped elements to achieve a basic band-pass filter response. Active transversal elements are used to sharpen the band-pass characteristic, and to overcome the high loss of MMIC lumped elements. Inductors have been realized with high-impedance transmission lines; spiral inductors may be substituted without a significant effect on performance.

II. Circuit Approach

A typical microwave transversal filter structure is shown in Fig. 1. In such a filter, multiple amplitude elements (transversal elements) are combined 180° out of phase. The phase delay is provided by 90° line lengths on the input and output sides [5], [6]. The outputs of the amplitude elements add constructively or destructively, depending on frequency. By appropriate selection of the number of transversal elements, and by tailoring their amplitudes, a wide range of passband characteristics may be realized. Because of the nature of this filter approach, parasitic (harmonic) passbands are present. Generally, a large number of transversal elements are required to achieve reasonable filter response. On the order of 25 transversal elements and 12.5 wavelengths of transmission line would be required in order to achieve the same level of performance

Manuscript received May 5, 1989; revised July 27, 1989.

The authors are with the Research Division, Raytheon Company, 131 Spring Street, Lexington, MA 02173.

IEEE Log Number 8930938.

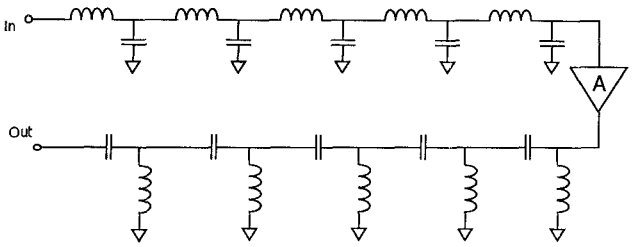

Fig. 2. The lumped element portion of the filter, consisting of a low-pass filter, an active gain element, and a high-pass filter in cascade.

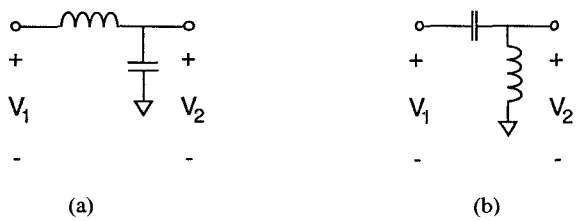

Fig. 3. Single-section (a) delay line and (b) advance line.

that is demonstrated by the filter presented in this paper. The size of such a filter would be inappropriate for MMIC implementation.

The filter presented in this paper utilizes both transversal and lumped element filtering. Lumped filter elements provide basic band-pass response. Transversal elements are also used. The constructive and destructive addition of multiple signals is used to enhance the filter characteristic.The lumped element portion of the filter is shown in Fig. 2. A conventional low-pass filter is used on the input. This is followed by a gain element, and then by a conventional high-pass filter. The characteristic of this filter is that of a conventional lumped element band-pass filter, with some added gain. The phase characteristics of this circuit may, however, be used to advantage.

The low-pass filter may be thought of as a delay line. For a single-delay line section, as in Fig. 3(a), the ratio of input to output voltages is

$$\frac{V_1}{V_2} = \sqrt{1-\omega^2 LC}\left[\sqrt{1-\omega^2 LC} + j\omega\sqrt{LC}\right]. \quad (1)$$

For $\omega^2 LC \leq 1$, this relationship may be rewritten as

$$\frac{V_1}{V_2} = (1-\omega^2 LC) + j\omega\sqrt{LC(1-\omega^2 LC)}\,. \quad (2)$$

It can be seen that a cutoff frequency may be defined as $\omega_c = 1/\sqrt{LC}$ and that the phase relationship between the input and output voltages of the low-pass section may be written as

$$\theta_{lp} = \sin^{-1}(\omega\sqrt{LC}). \quad (3)$$

This phase relationship has been plotted over normalized frequency in Fig. 4. As can be seen, phase delay is small at low frequency, and approaches 90° as cutoff is approached.

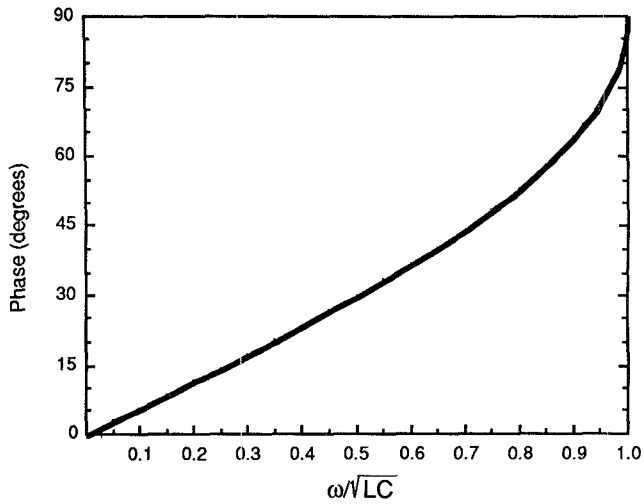

Fig. 4. Phase characteristic of a single-section delay line.

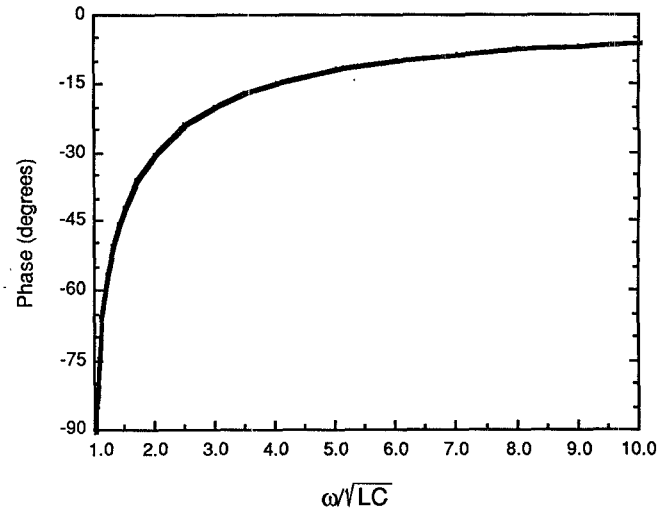

Fig. 5. Phase characteristic of a single-section advance line.

Similar calculations can be done for the high-pass section in Fig. 3(b), which may be thought of as a phase advance line. The ratio of input to output voltages is

$$\frac{V_1}{V_2} = \sqrt{1-\frac{1}{\omega^2 LC}}\left[\sqrt{1-\frac{1}{\omega^2 LC}} + \frac{1}{j\omega\sqrt{LC}}\right]. \quad (4)$$

For $\omega^2 LC \geq 1$, this relationship may be rewritten as

$$\frac{V_1}{V_2} = \left(1-\frac{1}{\omega^2 LC}\right) - j\sqrt{\frac{1}{\omega^2 LC}\left(1-\frac{1}{\omega^2 LC}\right)}. \quad (5)$$

It can be seen that a cutoff frequency may once again be defined as $\omega_c = 1/\sqrt{LC}$ and that the phase relationship between the input and output voltages of the low-pass section may be written as

$$\theta_{hp} = -\sin^{-1}\left(\frac{1}{\omega\sqrt{LC}}\right). \quad (6)$$

This phase relationship has been plotted over normalized frequency in Fig. 5. As can be seen, phase delay is

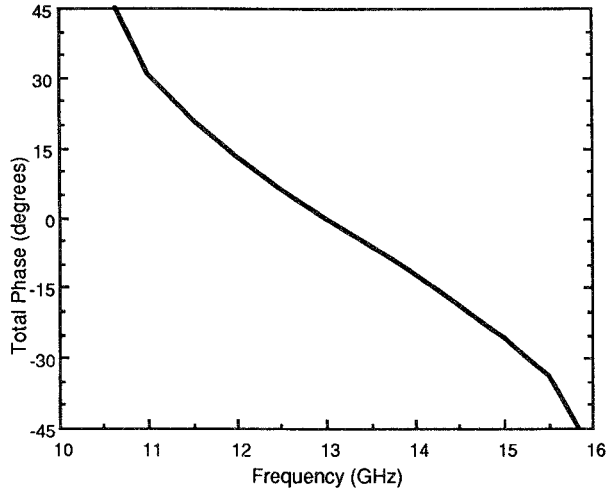

Fig. 6. Phase characteristic of the single-section delay line plus single-section advance line example.

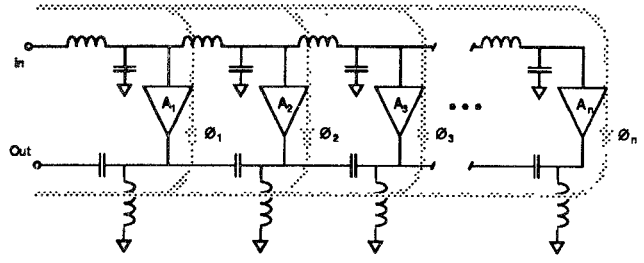

Fig. 7. Structure of a lumped and transversal element filter.

negative (therefore is a phase advance). It is small at high frequency and approaches $-90°$ as cutoff is approached.

The filter approach presented in this paper takes advantage of the combined phase delay of high-pass and low-pass sections. As an example, a low-pass section and a high-pass section have been designed. The low-pass section consists of a 0.5 nH inductor and a 0.2 pF capacitor and has a cutoff frequency of 15.9 GHz. The high-pass section consists of a 0.3 pF capacitor and a 0.75 nH inductor and has a cutoff of 10.6 GHz. The sum of the insertion phase (positive phase advances and negative phase delay) of these sections is plotted in Fig. 6. At 13 GHz (the middle of the frequency band between the upper and lower cutoffs) total insertion phase is 0°. Insertion phase deviates significantly from 0° as either cutoff frequency is approached. This frequency-dependent phase deviation is utilized to achieve transversal filtering in the filter presented in this paper.

The block diagram of the complete lumped and transversal element filter is shown in Fig. 7. The main signal path is through the last gain element, A_n. Lower amplitude gain elements are used for A_1 through A_{n-1}. Each gain element (A_x) has an insertion phase from input to output (ϕ_x) for its signal contribution. It is the deviation of any insertion phase element (ϕ_x) from the insertion phase of the main signal path (ϕ_n) that allows transversal filtering to take place. Wherever the difference between ϕ_x and ϕ_n is 180° or near 180°, substantial signal amplitude reduction is possible. This is similar to conventional

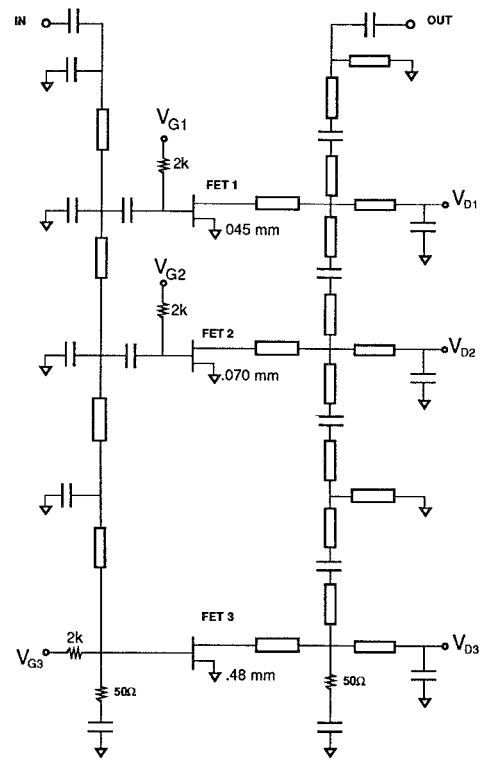

Fig. 8. Schematic for the lumped and transversal element band-pass filter example.

transversal filtering. The difference in phase increases as either cutoff is approached (see Fig. 6); therefore transversal filtering can readily be utilized to enhance the cutoff characteristics of the lumped element filter.

Since the basic filter passband characteristic is determined by lumped elements, very few transversal elements are required to produce a filter with sharp cutoff characteristics. Further, the transversal elements are relied on to achieve the sharp cutoff characteristics; therefore low-Q lumped elements can be tolerated.

III. Design Example

The schematic of the demonstrated band pass filter is shown in Fig. 8. The basic structure of Fig. 7 is used. This filter could accommodate up to four transversal elements, even though only two are needed to achieve adequate performance.

The design procedure begins with the design of the lumped element low-pass and high-pass filters. Conventional nine-element Chebychev filters are used for each. The low-pass filter is designed for the desired upper passband cutoff; the high-pass filter is designed for the desired lower passband cutoff. The two filters are cascaded through a single FET. Since this FET is in the signal path, it determines filter gain. In order to maximize gain, it is desirable to maximize the periphery of the FET. The periphery of this FET is limited by the last shunt capacitor in the input low-pass filter. Since the FET has considerable gate capacitance, the FET is sized so that its gate capacitance replaces the last shunt capacitor. Note that the first shunt inductor in the output high-pass filter must be

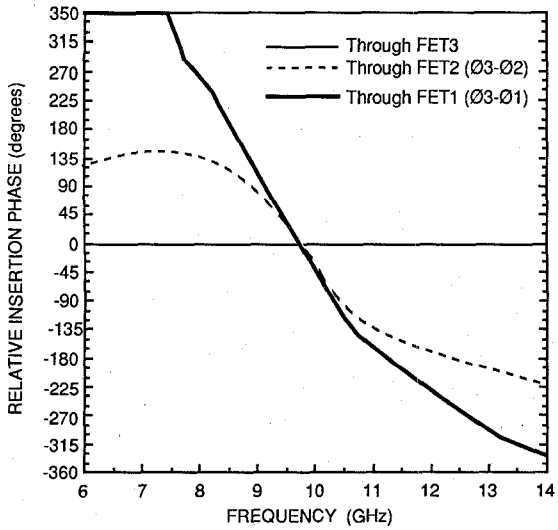

Fig. 9. Relative insertion phases through each FET of the lumped and transversal band-pass filter example.

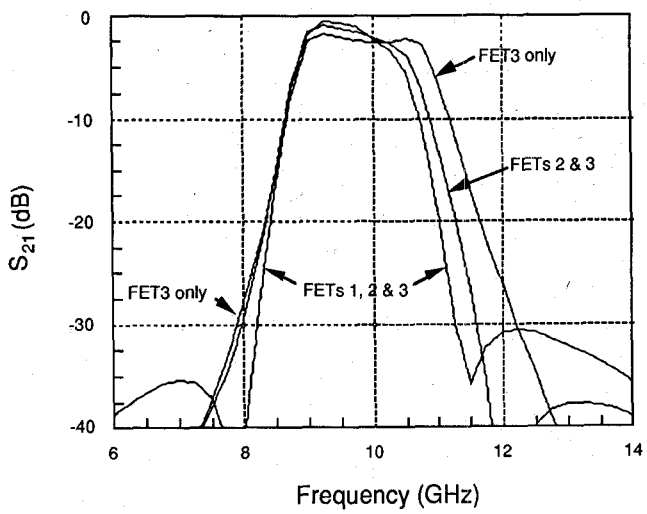

Fig. 10. Predicted band-pass characteristics of the filter example with all, some, and no transversal elements.

adjusted to compensate for the drain capacitance of the FET. Also note that both the low-pass and high-pass filters are terminated by a 50 Ω resistor. This ensures that both lumped element filters are properly matched. Further, it ensures the stability of the FET over a very wide frequency range. This completes the design of the lumped element portion of the filter. The filter, as is, provides a reasonable band-pass filter characteristic, although without sharp cutoff skirts.

The design of the transversal elements can proceed, given the guidelines of Section II above. In order to demonstrate the potential for transversal filtering, the insertion phases of the signal paths through FET1, FET2, and FET3 were determined (using conventional modeling software). Since the main signal path (ϕ_3) is through FET3, it is most revealing to express the phases of the other signal paths relative to ϕ_3. Fig. 9 shows the insertion phase difference for FET2 ($\phi_3 - \phi_2$) and for FET1 ($\phi_3 - \phi_1$). It is apparent that the signal path through FET1 can

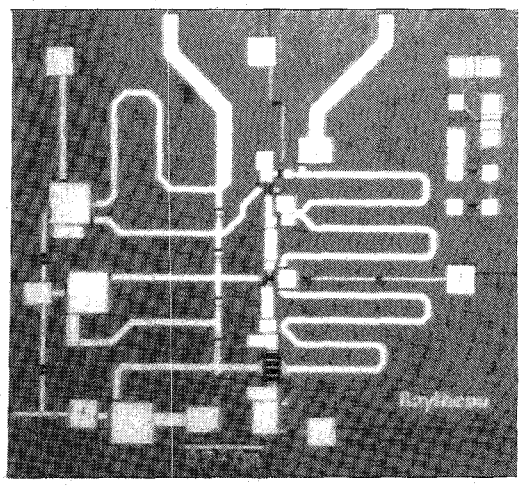

Fig. 11. Photograph of the 9.8–11.1 GHz band-pass filter MMIC.

offer complete signal cancellation near 8.5 GHz at the lower cutoff, and near 11.25 GHz at the higher cutoff. Similarly, the path through FET2 offers complete cancellation near 12.25 GHz at the high-end cutoff, and partial cancellation over the 7–8 GHz band at the lower cutoff (since 180° phase difference is not fully achieved).

The predicted performance for the filter is summarized in Fig. 10. Three curves are shown: one (labeled FET3 only) shows the filter with no transversal elements, one (labeled FET's 2 and 3) with partial transversal elements, and the last (labeled FET's 1, 2, and 3) for the complete filter with all elements. When no transversal elements are used, conventional band-pass filter performance is expected. This is the case represented in Fig. 2. When the transversal elements are added, the band edge rejection skirts are sharpened considerably. Note that the transversal elements limit ultimate filter rejection (far from the band edges), in return for improvements in rejection on the skirts. In the case of the filter presented in this paper, a 30 dB ultimate rejection goal was used.

IV. MMIC Fabrication

The filter was fabricated as an MMIC and is shown in Fig. 11. Inductive elements are implemented with high-impedance transmission line sections. The capacitors are made with a 2000 Å silicon nitride dielectric. The transversal elements are standard low-current, ion-implanted FET's with 0.5 μm gates and 3×10^{17} cm^{-3} doping. All bias circuitry is included on chip. Each FET has a drain bias circuit, implemented through the shunt inductors of the high-pass filter. The drain biases are tied together on chip, but since the connections are made through air bridges, they are readily separated. This is useful for performance diagnosis, and is not generally used. The gates are individually biased through 2 kΩ resistors, although they are generally biased by a common voltage. The wafer was thinned to 4 mils and 20×100 μm^2 vias holes were etched. The complete MMIC measures 70×75 mils^2 (1.8×1.9 mm^2), including some area taken up by optional test patterns. Chip size could be further reduced by removing

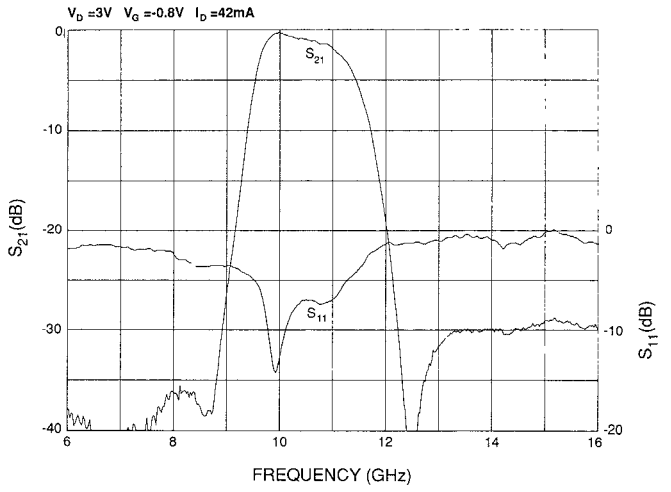

Fig. 12. Measured performance of the 9.8–11.1 GHz band-pass filter MMIC.

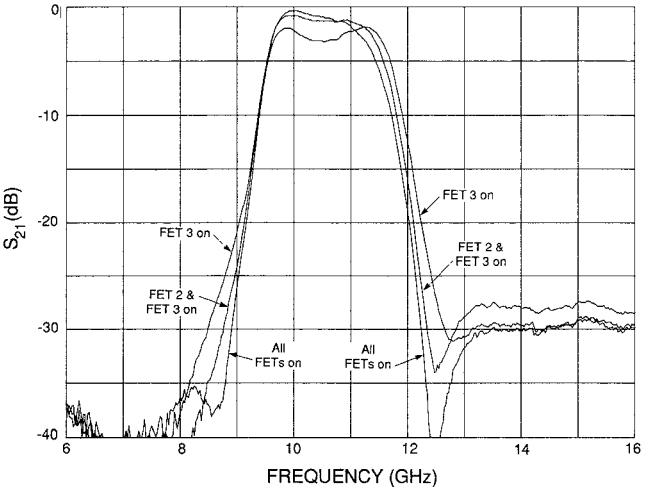

Fig. 13. Measured performance of the 9.9–11.1 GHz band-pass filter in normal operation, and when some FET's are turned off.

the test patterns and replacing some high-impedance line sections with spiral inductors.

V. Measured Performance

The measured performance of the filter is shown in Fig. 12. Passband loss is 2 dB, with 1 dB ripple. For a strictly passive lumped element filter, the passband loss would be on the order of 9 dB. The active transversal elements reduce the loss by approximately 7 dB. Rejection exceeding 30 dB is achieved 1.0 GHz from the lower passband edge, 1.1 GHz from the upper passband edge. Modeling shows that with a conventional lumped element filter such rejection could at best have been achieved 2.2 GHz from the passband edges. Return loss is 5 dB or better within the passband, and approaches 0 dB outside of the passband, as would be expected from a lumped element filter. The FET's in the filter are biased at 3 V on the drain, and -0.8 V on all gates ($\sim 40\% I_{dss}$). Performance is essentially unaffected over a drain voltage range of 2.5 to 7 V. Current consumption is 42 mA, so at 3 V power consumption is only 126 mW.

In order to confirm the contributions of the transversal elements, separate biases were provided to each FET, allowing each of their gains to be removed. This was done by reducing drain bias to 0 V and gate voltage to beyond pinch-off (-4 V). This allows most of the effect of any given FET to be removed, but since a substantial capacitive path still exists from gate to drain (~ 0.3 pF/mm), the effect of any FET cannot be completely removed. The results of this experiment are shown in Fig. 13. The curve labeled "all FET's" is the same as S_{21} in Fig. 12. The other two curves indicate the performance when FET1 is turned off and when both FET's 1 and 2 are turned off. FET's 1 and 2 do not contribute much gain, so the passband loss does not change significantly. Note that the cutoff frequencies are not significantly changed when FET1 and FET2 are turned off, but near in rejection degrades substantially.

Fig. 13 shows measured performance curves which may be directly compared to the predicted curves in Fig. 10. The major difference between the measured and predicted curves is a shift in the passband of approximately 0.5 GHz, indicating errors in the models of some of the lumped elements. The passband shape, the rejection shape, and filter rejection are all modeled quite accurately. The effect of the transversal elements is confirmed in the measurements, even though it is not possible to fully remove the transversal elements.

VI. Summary

A novel filter structure has been described using a combination of lumped and transversal elements. The resulting filter yields performance superior to that which can be achieved with lumped elements alone, and in a much smaller size than could be realized with transversal elements alone. A 9.8–11.1 GHz MMIC band-pass filter was designed and fabricated to demonstrate the concept.

Although only a passband filter was shown, the concept can readily be extended to include low-pass filters, high-pass filters, and diplexers. Similar circuitry can be envisioned to include recursive elements.

Acknowledgment

The authors would like to thank K. Simon for analytical assistance, P. Hindle for MMIC process coordination, A. Platzker and R. Pucel for helpful discussions, and D. Kelly for assistance in evaluation.

References

[1] W. Titus and M. Miller, "2–26 GHz MMIC frequency converter," in *Proc. IEEE GaAs IC Symp.*, Nov. 1988, pp. 181–184.
[2] J. Culver, D. Zimmerman, and C. Panasik, "A 32 tap digitally controlled programmable transversal filter using LSI GaAs ICs," in *IEEE MTT-S Int. Microwave Symp. Dig.*, May 1988, pp. 561–564.
[3] C. Rauscher, "Microwave active filters based on transversal and recursive principles," *IEEE Trans. Microwave Theory Tech.*, vol. MTT-33, pp. 1350–1360, Dec. 1985.
[4] E. Strid, "A monolithic 10 GHz vector modulator," in *Proc. IEEE GaAs IC Symp.*, Oct. 1983, pp. 109–112.
[5] G. Wagner, "High bandwidth transversal filter," U.S. Patent 4 291 286.

[6] W. Jutzi, "Microwave bandwidth active transversal filter concept with MESFET's," *IEEE Trans. Microwave Theory Tech.*, vol. MTT-19, pp. 760–767, Sept. 1971.

✠

Manfred J. Schindler (S'80-M'82) was born in Vienna, Austria, in 1957. He received the B.S. degree in electrical engineering from Columbia University, New York City, in 1979, and the M.S. degree in electrical and computer engineering, concentrating in microwave engineering, from the University of Massachusetts, Amherst, in 1982.

Upon completing his undergraduate studies he joined the Raytheon Company, Equipment Division, where he worked on communications-related RF and microwave circuitry. He entered the University of Massachusetts in 1980, and returned to Raytheon in 1981, where he worked on *X*-band MIC's and *Q*-band IMPATT power amplifiers. Since 1984 he has been with the Raytheon Research Division, Lexington, MA, where he is presently manager of the MMIC Design group in the Semiconductor Laboratory. He has been involved in the development of a variety of microwave and millimeter-wave GaAs monolithic circuits, particularly for broad-band applications.

✠

Yusuke Tajima (M'79) received the B.S. and Ph.D. degrees from Tokyo University in electronics engineering in 1970 and 1980, respectively. His thesis dealt with GaAs FET's and their applications.

Before joining the Raytheon Research Division, Lexington, MA, in 1979, he was a Senior Engineer with the Toshiba Cooperation in Kawasaki, Japan, where he supervised the development of high-power GaAs FET's and GaAs FET amplifiers. From 1974 to 1975, he was employed at the Raytheon Research Division as an exchange engineer. In 1979, he returned to Raytheon, where he is now a member of the Research Division Semiconductor Laboratory. He has technical and program management responsibilities over monolithic circuit and GaAs device development. He is also the author of a number of technical papers in Japanese and English.